Optimized Resource Allocation for Distributed Joint Radar-Communication System

Ammar Ahmed, *Member, IEEE*, and Yimin D. Zhang, *Fellow, IEEE*

***Abstract*—In this paper, we consider a distributed joint radar-communication (JRC) multiple-input multiple-output (MIMO) system that performs both radar and communication objectives simultaneously. By introducing radar and communication performance metrics, optimized power allocation is achieved for different transmitters of the JRC system. The objective of the radar subsystem is to achieve a desired target localization accuracy quantified in terms of the Cramer-Rao bound of the location estimates, whereas the objective of the communication subsystem is to improve the classical Shannon capacity. First, we consider non-cooperative radar- and communication-centric operations, and the power allocations are respectively optimized for these cases. Next, we present two novel resource allocation strategies for the cooperative JRC system. In the first strategy, joint resource optimization for radar and communication subsystems is performed by exploiting the same waveform resources, resulting in high spectrum efficiency. The second approach provides enhanced flexibility by exploiting separate sets of waveforms that are respectively dedicated to the radar and communication subsystems, enabling the JRC system to independently change radar subsystem waveforms based only on the radar surveillance profile, without impacting the communication subsystem waveforms. Simulation results clearly demonstrate significant performance gain of the proposed cooperative JRC system over radar- or communication-centric power allocation schemes.**

Keywords: Joint radar-communications, distributed MIMO radar, power allocation, target localization, Shannon capacity.

I. Introduction

Spectrum sharing has attracted significant research attention in the past decade due to the ongoing congestion of spectral resources [1–5]. Modern communication systems require the expansion of existing spectral allocations in order to support higher data rates. Moreover, emerging technical innovations, like Internet-of-Things, require new frequency allocations for their successful deployment. In this context, significant efforts have been made in the field of cognitive radios to efficiently manage the utilization of frequency bands [6]. Recently, the coexistence of multiple applications within the same frequency bands has been proposed to mitigate the spectral congestion problem by simultaneously sharing the same spectral resources for multiple applications [7–11]. Joint radar-communications (JRC) is an important example of such systems that perform the secondary communication operation in addition to the primary radar function while utilizing the same frequency resources [4, 12–20]. Recent studies have also investigated the applications of radar-communication spectrum sharing in context of parameter estimation problems [21–23].

In JRC systems, the transmitted waveform satisfies the objectives of both radar and communication subsystems. The radar function is considered to be the principal objective of the JRC system whereas the communication operation is secondary. Different types of JRC systems have been discussed in the literature and can be loosely divided into three main categories [4, 5]. The first type of JRC system employs a single transmit antenna that broadcasts dual-purpose waveforms performing radar and communication operations. The performance of such systems has been rigorously discussed in the literature by exploiting waveform diversity [12] or popular communication waveforms [7, 24–28]. The second type of JRC system consists of a transmit antenna array that employs adaptive beamforming along with waveform diversity to transmit different sensing and information streams respectively towards radar and communication directions [5, 14–17, 19, 20]. Finally, the third type of JRC system consists of distributed transmitters and receivers that collectively perform radar and communication tasks simultaneously [29–32].

Resource allocation for JRC systems has recently become a topic of great research interest. For single transmitter-based JRC systems, the resource allocation problem was addressed by optimizing the transmit power of different subcarriers depending on the propagation channels of radar and communication users [4, 24–26]. In beamforming-based JRC systems where the number of hardware up-conversion chains is far less than the number of available transmit antennas, resource allocation was discussed in terms of the optimized antenna selection profile by exploiting convex optimization approaches [4, 5, 33, 34].

In our previous study on distributed JRC [4, 29, 30], we exploited target localization error minimization and water-filling approach to carry out power allocation for joint radar and communication transmission. In this paper, we respectively exploit Cramer-Rao bound (CRB) and Shannon capacity as the radar and communication system objectives, and both sum and worst-case communication capacities are considered. In the proposed approaches, both radar and communication functions can share the transmit waveforms, or separate waveforms can be designed so that they are dedicated to their respective functions.

Reference [31] studied a distributed JRC scheme with a

This work was supported in part by National Science Foundation (NSF) under Grant No. ECCS-2236023. (Corresponding author: Y. D. Zhang.)

A. Ahmed was with the Department of Electrical and Computer Engineering, Temple University, Philadelphia, PA 19122. He is now with Aptiv, Agoura Hills, CA 91301. (email: ammar.ahmed@aptiv.com)

Y. D. Zhang is with the Department of Electrical and Computer Engineering, Temple University, Philadelphia, PA 19122. (email: ydzhang@temple.edu)

focus on minimizing the probability of intercept. It exploits the same signal model as in [4, 29] and, unlike this work, it does not address the design and analysis of radar and communication objectives, nor does it consider the shared or dedicated waveform concept. A heterogeneous co-existing radar and communication approach for distributed communication and colocated MIMO radars is presented in [35]. On the other hand, our approach considers a shared physical platform that serves both radar and communication objectives and, as a result, inherently enjoys reduced coupling between radars and communications.

Multiple-input multiple-output (MIMO) radar systems with widely distributed antennas are well-known to offer improved localization capabilities due to their enhanced spatial spread [36]. Extensive studies on distributed MIMO radars are available that address target localization accuracy based on the transmit power, bandwidth, as well as the number and the locations of transmit and receive antennas [37, 38]. Resource-aware designs are very important in order to reduce the operational cost and achieve optimized performance of sensor nodes or antennas in the network.

The participating radars in distributed radar networks can be connected with ground stations, fusion centers, or in a distributed fashion using wireless links. Therefore, modern distributed radars need to perform the radar and communication functions simultaneously while considering the on-site resource constraints. Moreover, resource-aware distributed and multi-layered platforms, such as unmanned aerial network (UAV) networks, also desire simultaneous sensing and communication operations exploiting the same hardware and waveform resources.

In this paper, we propose novel optimized resource-aware strategies for distributed JRC MIMO systems that provide improved performance of both radar and communication subsystems. Our contributions are summarized as follows:

- We present radar and communication quality metrics for distributed JRC systems that can be exploited to simultaneously optimize power allocation and achieve improved system performance. Subsequently, power allocation for radar- and communication-centric operations is presented that serves as the baseline for the evaluation of cooperative JRC system performance.
- We develop a strategy to optimize cooperative power allocation for JRC system where both radar and communication subsystems share the same waveform resources to satisfy their goals resulting in high spectrum efficiency.
- We extend the distributed JRC power allocation scheme for the case where radar and communication subsystems respectively exploit their dedicated waveforms. By using this strategy, the JRC system enjoys the flexibility of changing the radar waveform depending on the surveillance profile of the radar subsystem.
- For all the proposed power allocation strategies, we provide mathematical formulations that enable sum- as well as worst-case Shannon capacity optimization for the communication subsystem while successfully achieving the desired localization performance for the radar subsystem.

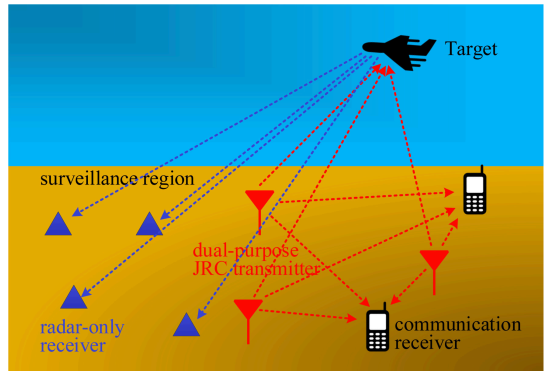

Fig. 1: Distributed JRC MIMO system showing one target, three dual-purpose transmitters, four radar receivers, and two communication receivers.

The rest of the paper is organized as follows. Signal models and necessary preliminaries are introduced in Section II. In Section III, we present the performance metrics that enable power allocation strategies for distributed JRC system. Optimized power allocation for radar- and communication-centric operations is considered in Section IV and serves as the baseline for the performance evaluation of the cooperative JRC systems. Power allocation for the cooperative JRC system exploiting shared or dedicated waveform resources is presented in Section V. Section VI illustrates an example of information embedding strategy for the distributed JRC system that enables the transfer of communication information. Simulation results are presented in Section VII, whereas Section VIII concludes the paper.

Notations: We use lower-case and upper-case bold letters to represent vectors and matrices, respectively. In particular, $\mathbf{1}_M$ denotes a column vector of length M consisting of all ones. The superscripts $(\cdot)^{\mathrm{T}}$, $(\cdot)^{\mathrm{H}}$, and $(\cdot)^*$ represent the transpose, conjugate transpose, and conjugate operators, respectively, whereas $\mathbb{E}\{\cdot\}$ shows the expectation operator. Moreover, the notation $[\mathbf{A}]_{k,l}$ denotes the element on kth row and lth column of matrix $\mathbf{A}$, and $\psi \in \mathbf{\Psi}$ represents an element ψ that is the member of set $\mathbf{\Psi}$. Furthermore, $|\cdot|$ returns an absolute value and $\log(\cdot)$ denotes base-2 logarithm.

II. Distributed JRC System Model

Consider a distributed JRC MIMO system consisting of M dual-purpose transmitters, N radar receivers, and R communication receivers arbitrarily located in a two-dimensional (2-D) coordinate system at locations $(x_{m_{\mathrm{tx}}}, y_{m_{\mathrm{tx}}})$, $(x_{n_{\mathrm{rx}}}, y_{n_{\mathrm{rx}}})$, and $(x_{r_{\mathrm{com}}}, y_{r_{\mathrm{com}}})$, respectively, where $1 \leq m \leq M$, $1 \leq n \leq N$, and $1 \leq r \leq R$. Fig. 1 illustrates the distributed JRC MIMO system.

The transmitters emit dual-purpose waveforms that serve the objectives of both radar and communication subsystems. Denote $p_{m_{\mathrm{tx}}}$ as the transmit power of the mth transmitter, and $p_{m_{\mathrm{tx,min}}}$ and $p_{m_{\mathrm{tx,max}}}$ the minimum and maximum allowable powers that can be transmitted from this transmitter. We express the actual, minimum, and maximum possible transmit powers of all the JRC transmitters in the vector form, each having a size of $M \times 1$, as follows:

$$\begin{aligned}\mathbf{p}_{\text{tx}} &= [p_{1_{\text{tx}}}, p_{2_{\text{tx}}}, \ldots, p_{M_{\text{tx}}}]^{\text{T}},\\ \mathbf{p}_{\text{tx,min}} &= [p_{1_{\text{tx,min}}}, p_{2_{\text{tx,min}}}, \ldots, p_{M_{\text{tx,min}}}]^{\text{T}},\\ \mathbf{p}_{\text{tx,max}} &= [p_{1_{\text{tx,max}}}, p_{2_{\text{tx,max}}}, \ldots, p_{M_{\text{tx,max}}}]^{\text{T}}.\end{aligned} \tag{1}$$

Furthermore, we denote $P_{\text{total}_{\max}}$ as the maximum allowable power that can be transmitted from all JRC transmitters collectively, such that

$$\sum_{m=1}^{M} p_{m_{\text{tx}}} = \mathbf{1}_M^{\text{T}} \mathbf{p}_{\text{tx}} = P_{\text{total}} \leq P_{\text{total}_{\max}}. \tag{2}$$

The signal model of the radar and communication subsystems are respectively discussed in the following two subsections.

A. Radar subsystem

The radar subsystem acts as a distributed MIMO radar system whose primary objective is to detect targets and track their locations. Assume an extended target composed of a collection of several point scatterers. According to [37, 39], the target return for this case can be approximated by a point scatterer having a center of mass at location (x, y) if the target is moving slowly. The complete information of the target is determined by the distance between the target and to MIMO transmitters, the distance between the target and the receivers, and the radar cross-section (RCS) that measures the detectability of the target by the radar subsystem. The RCS is given by $h_{m,n}$ for the path traversed by the waveform from the mth transmitter to the target and back to the nth radar receiver of the distributed MIMO system.

The effective range between the target and the mth transmitter can be given as

$$D_{m_{\text{tx}}} = \sqrt{(x - x_{m_{\text{tx}}})^2 + (y - y_{m_{\text{tx}}})^2}, \tag{3}$$

whereas the range between the target and the nth receiver is given as

$$D_{n_{\text{rx}}} = \sqrt{(x - x_{n_{\text{rx}}})^2 + (y - y_{n_{\text{rx}}})^2}. \tag{4}$$

The propagation delay $\tau_{m,n}$ due to the propagation path from the mth transmitter to the target and from the target to the nth receiver is expressed as

$$\tau_{m,n} = \frac{D_{m\text{tx}} + D_{n\text{rx}}}{c}, \tag{5}$$

where c is the propagation velocity of the transmitted signals.

During each radar pulse, the mth dual-purpose transmitter radiates an orthogonal waveform $s_m(t)$ which ideally tends to satisfy

$$\frac{1}{T}\int_0^T s_{m_1}(t-\zeta_1) s_{m_2}^*(t-\zeta_2)\mathrm{d}t \approx \begin{cases} 1, & m_1 = m_2,\ \zeta_1 = \zeta_2,\\ 0, & m_2 \neq m_2,\end{cases} \tag{6}$$

for $m_1, m_2 = 1, \cdots, M$, where T is the duration of a pulse, t is the fast time, and ζ_1 and ζ_2 are the propagation delays. The autocorrelation between the delayed versions of the waveforms is ideally close to zero only if the ratio $1/|\zeta_1 - \zeta_2|$ is less than the bandwidth. Note that there are several available methods that can be used to design appropriate waveforms for distributed MIMO radar as well as for wireless communications [40–42].

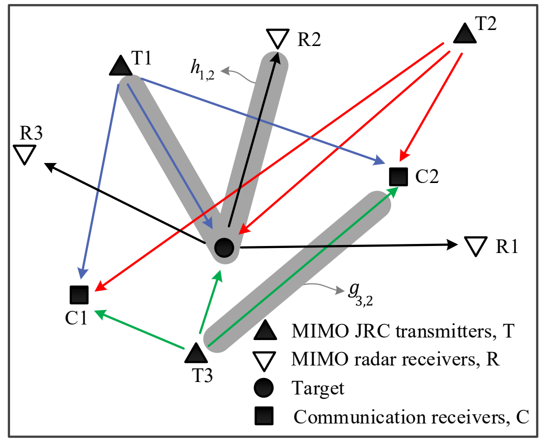

Fig. 2: A distributed JRC MIMO system illustrated with three dual-purpose transmitters, three radar receivers, and two communication receivers.

The estimation of the target location can be done either in a coherent or non-coherent manner. Coherent processing considers the synchronization of both phase and time for distributed MIMO transmitters and receivers, whereas non-coherent processing only relies on time synchronization [37]. Without loss of generality, we consider the latter and assume the case where the JRC transmitters and the radar receivers are not required to be phase synchronized. In this case, the time delay information of the target is achieved from the variations in the envelope of the transmit signals. For non-coherent case, the radar return signal transmitted by the mth transmitter, reflected by the target, and received at the nth receiver is expressed as:

$$s_{m,n}^{\text{rad}}(t) = \sqrt{\alpha_{m,n} p_{m_{\text{tx}}}} h_{m,n} s_m(t - \tau_{m,n}) + w_{m,n}^{\text{rad}}(t), \tag{7}$$

where $w_{m,n}^{\text{rad}}(t) \sim \mathcal{CN}(0, \sigma_w^2)$ represents the circularly symmetric zero-mean complex white Gaussian noise. Moreover, $\alpha_{m,n}$ represents the signal variation due to path loss effects, given by [39]

$$\alpha_{m,n} = \frac{\lambda^2}{(4\pi)^3 D_{m_{\text{tx}}}^2 D_{n_{\text{rx}}}^2}, \tag{8}$$

where λ is the signal wavelength.

In general, radar operations are considered to have search mode and track mode. In the search mode, no channel state information is assumed and, in particular, new targets need to be detected and localized. In the track mode, the previous states of all targets are known and the system updates their new positions and the associated channels over time [43]. To focus on the optimized resource allocation, we assume that the target RCS $h_{m,n}$ and the location of the target (x, y) are known or estimated by the JRC system and are updated over time.

B. Communication subsystem

We can express the signal transmitted by the mth JRC transmitter and received at the rth communication receiver

$(1 \leq r \leq R)$ as

$$s_{m,r}^{\rm com}(t) = \sqrt{\beta_{m,r} p_{m_{\rm tx}}} g_{m,r} s_m(t-\kappa_{m,r}) + w_{m,r}^{\rm com}(t). \quad (9)$$

Here, $g_{m,r}$ denotes the complex channel gain between the mth JRC transmitter and the rth communication receiver, $\kappa_{m,r}$ is the respective propagation delay, and $\beta_{m,r} \propto \bar{D}_{m,r}^{-2}$ incorporates the path loss effects, where $\bar{D}_{m,r}$ is the distance between the mth transmitter and the rth communication receiver, given by

$$\bar{D}_{m,r} = \sqrt{(x_{r_{\rm com}} - x_{m_{\rm tx}})^2 + (y_{r_{\rm com}} - y_{m_{\rm tx}})^2}. \quad (10)$$

We assume $w_{m,r}^{\rm com}(t) \sim \mathcal{CN}(0, \bar{\sigma}_{m,r}^2)$ to be circularly complex white Gaussian noise whose statistics are known at the transmitters. The channel state information, expressed as the complex channel gain vector $\mathbf{g} = [g_{1,1}, g_{1,2}, \ldots, g_{M,1}, \ldots, g_{M,R}]^{\rm T}$, is also assumed known at the JRC transmitters and at the fusion center as this information can be initially obtained from the initial alignment stage of the communication subsystem and then kept tracked during its operation [44]. We also assume that the signals reflected from the target and received at each communication receiver have a significantly lower magnitude compared to the line-of-sight transmission from the transmitters and, thus, are ignored.

III. Performance Metrics

In this section, we discuss the performance metrics of the radar and communication subsystems that are used to address the resource allocation problem for the distributed JRC MIMO system. Our objective is to optimally allocate the maximum available power among the JRC dual-purpose transmitters.

A. Radar subsystem

The radar subsystem performance is evaluated in terms of the CRB representing the lower bound on the mean squared error (MSE) of the target's location estimates. Define the unknown parameter vector $\boldsymbol{\theta} = [x, y, \mathbf{h}^{\rm T}]^{\rm T}$ where $\mathbf{h} = [h_{1,1}, \cdots, h_{1,N}, h_{2,1}, \cdots, h_{M,N}]^{\rm T}$. We assume that coarse estimates of $\boldsymbol{\theta}$ are available by the JRC system from the previous cycles. For the vector parameter $\boldsymbol{\theta}$, the CRB submatrix associated with the localization error can be expressed as [4, 37, 38]

$$\mathbf{C}_{x,y}(\mathbf{p}_{\rm tx}) = \left\{ \sum_{m=1}^{M} p_{m_{\rm tx}} \begin{bmatrix} q_{a_m} & q_{c_m} \\ q_{c_m} & q_{b_m} \end{bmatrix} \right\}^{-1}, \quad (11)$$

where

$$\begin{aligned} q_{a_m} =& \xi_m \sum_{n=1}^{N} \alpha_{m,n} |h_{m,n}|^2 \left(\frac{x_{m_{\rm tx}} - x}{D_{m_{\rm tx}}} + \frac{x_{n_{\rm rx}} - x}{D_{n_{\rm rx}}} \right)^2, \\ q_{b_m} =& \xi_m \sum_{n=1}^{N} \alpha_{m,n} |h_{m,n}|^2 \left(\frac{y_{m_{\rm tx}} - x}{D_{m_{\rm tx}}} + \frac{y_{n_{\rm rx}} - x}{D_{n_{\rm rx}}} \right)^2, \\ q_{c_m} =& \xi_m \sum_{n=1}^{N} \alpha_{m,n} |h_{m,n}|^2 \left(\frac{x_{m_{\rm tx}} - x}{D_{m_{\rm tx}}} + \frac{x_{n_{\rm rx}} - x}{D_{n_{\rm rx}}} \right) \\ & \cdot \left(\frac{y_{m_{\rm tx}} - x}{D_{m_{\rm tx}}} + \frac{y_{n_{\rm rx}} - x}{D_{n_{\rm rx}}} \right), \\ \xi_m =& 8\pi^2 B_m^2 / (\sigma_w^2 c^2), \end{aligned} \quad (12)$$

and B_m is the effective bandwidth of the signal transmitted from the mth transmitter. Following additional matrix manipulations, the trace of $\mathbf{C}_{x,y}(\mathbf{p}_{\rm tx})$ can be expressed as

$$\sigma_{x,y}^2(\mathbf{p}_{\rm tx}) = {\rm tr}\{\mathbf{C}_{x,y}(\mathbf{p}_{\rm tx})\} = \frac{\mathbf{q}^{\rm T}\mathbf{p}_{\rm tx}}{\mathbf{p}_{\rm tx}^{\rm T}\mathbf{A}\mathbf{p}_{\rm tx}}, \quad (13)$$

Here,

$$\mathbf{q} = \mathbf{q}_a + \mathbf{q}_b, \;\; \mathbf{A} = \mathbf{q}_a \mathbf{q}_b^{\rm T} - \mathbf{q}_c \mathbf{q}_c^{\rm T}, \quad (14)$$

such that $\mathbf{q}_a = [q_{a_1}, q_{a_2}, \ldots, q_{a_M}]^{\rm T}$, $\mathbf{q}_b = [q_{b_1}, q_{b_2}, \ldots, q_{b_M}]^{\rm T}$, and $\mathbf{q}_c = [q_{c_1}, q_{c_2}, \ldots, q_{c_M}]^{\rm T}$. For the case of uniform power allocation, i.e., $\mathbf{p}_{\rm tx} = \mathbf{1}_M$, the trace of the CRB matrix takes the form of $\sigma_{x,y}^2(\mathbf{p}_{\rm tx}) = \frac{1}{\bar{p}} \frac{\mathbf{q}^{\rm T}\mathbf{1}_M}{\mathbf{1}_M^{\rm T}\mathbf{A}\mathbf{1}_M}$, where $\bar{p} = \frac{1}{M} P_{\rm total}$ [38].

Since coarse estimates of $\boldsymbol{\theta}$ are known at the JRC system from the previous cycles, we can use these estimates to determine the localization MSE $\sigma_{x,y}^2(\mathbf{p}_{\rm tx})$ and subsequently optimize the power allocation profile of the JRC system. Meanwhile, the estimates of $\sigma_{x,y}^2(\mathbf{p}_{\rm tx})$ are continuously updated based on the signals reflected by the target and received at the radar receivers.

B. Communication subsystem

We assume that the channel state information of the communication receivers is known by the JRC MIMO system from the communication history and the waveforms transmitted from each JRC transmitter are broadcast to all intended communication receivers. Moreover, the waveforms used by the JRC MIMO system for the communication purpose are also assumed to be known at the communication receivers [15, 17, 29]. We use Shannon capacity, representing the maximum possible data rate that can be achieved, to evaluate the performance of the communication subsystem. The Shannon capacity between the mth JRC transmitter and the rth communication receiver is expressed as

$$\Re_{m,r} = \log\left(1 + \frac{\beta_{m,r}|g_{m,r}|^2 p_{m_{\rm tx}}}{\sigma_{m,r}^2}\right) = \log\left(1 + \frac{p_{m_{\rm tx}}}{\gamma_{m,r}}\right), \quad (15)$$

where $\gamma_{m,r} = \sigma_{m,r}^2 / (\beta_{m,r}|g_{m,r}|^2)$. The Shannon capacity is a theoretical limit that cannot be achieved in practice, but as link level design techniques improve, data rates for the additive white noise channels approach this theoretical bound [45].

We use two different types of performance metrics to evaluate the entire communication subsystem. The first metric is to maximize the sum capacity represented as

$$\Re_{\rm sum} = \sum_{r=1}^{R}\sum_{m=1}^{M} \Re_{m,r} = \sum_{r=1}^{R}\sum_{m=1}^{M} \log\left(1 + \frac{p_{m_{\rm tx}}}{\gamma_{m,r}}\right). \quad (16)$$

The problem of maximizing such sum capacity can also be represented as a least-squares optimization problem by employing the water-filling approach [4, 29].

When maximizing the sum capacity, it is possible that some communication receivers having poor channel conditions are completely ignored. This can lead to an undesirable situation for the users of critical importance. To mitigate this problem, in the second performance metric, we consider the worst-case capacity of the communication receivers. This criterion is expressed as

$$\Re_{\text{worst}} = \min_{r} \left(\sum_{m=1}^{M} \Re_{m,r} \right) = \min_{r} \left(\sum_{m=1}^{M} \log \left(1 + \frac{p_{m_{\text{tx}}}}{\gamma_{m,r}} \right) \right). \tag{17}$$

Worst-case Shannon capacity is an important metric for communication systems involving critical infrastructure that cannot tolerate being ignored in case they have poor channel conditions. However, when this metric is used, a significant portion of the resources may be drained in communication channels that have poor conditions. Therefore, design engineers should be cautious when choosing the performance metrics for the JRC systems.

IV. Optimized Power Allocation for Individual Radar and Communication Systems

In this section, we discuss the optimized power allocation for the scenario when the complete system is dedicated to either the radar or the communication task. It results in optimized power allocation for the cases when either the radar or the communication function is considered to have a dominant priority. The performance achieved for these cases can serve as a baseline for comparison with the performance achieved by the JRC system.

A. Radar-only operation

The optimal power allocation for radar-only operation can be expressed as follows [38]:

$$\begin{aligned} \min_{\mathbf{p}_{\text{tx}}} \quad & \sigma^2_{x,y}(\mathbf{p}_{\text{tx}}) \\ \text{subject to} \quad & \mathbf{p}_{\text{tx,min}} \leq \mathbf{p}_{\text{tx}} \leq \mathbf{p}_{\text{tx,max}}, \\ & \mathbf{1}_M^{\text{T}} \mathbf{p}_{\text{tx}} \leq P_{\text{total}_{\max}}. \end{aligned} \tag{18}$$

The objective function $\sigma^2_{x,y}(\mathbf{p}_{\text{tx}})$ used in the above optimization problem is non-convex. Following the procedure used in [38], we first replace $\min_{\mathbf{p}_{\text{tx}}}[\sigma^2_{x,y}(\mathbf{p}_{\text{tx}})]$ with $\max_{\mathbf{p}_{\text{tx}}}[\sigma^2_{x,y}(\mathbf{p}_{\text{tx}})]^{-1}$. Using Eq. (13) and the subsequent discussion on $\sigma^2_{x,y}(\mathbf{p}_{\text{tx}})$, problem (18) can be converted into the following convex form:

$$\begin{aligned} \max_{\mathbf{p}_{\text{tx}}} \quad & \mathbf{q}^{\text{T}} \mathbf{p}_{\text{tx}} \\ \text{subject to} \quad & \mathbf{p}_{\text{tx,min}} \leq \mathbf{p}_{\text{tx}} \leq \mathbf{p}_{\text{tx,max}}, \\ & \mathbf{1}_M^{\text{T}} \mathbf{p}_{\text{tx}} \leq P_{\text{total}_{\max}}. \end{aligned} \tag{19}$$

The optimization problem (19) tends to minimize the localization MSE for the distributed MIMO radar such that the maximum available power is utilized. The optimal solution to problem (19) can be further used as the starting point of a local optimization algorithm applied to the original non-convex problem (18) [38]. In this case, the radar subsystem achieves the best localization performance as the maximum transmit power is optimally allocated to the transmitters, resulting in the lowest localization MSE given by η_{opt}.

Unlike the above optimization strategy where all the available power is used for the radar task, resulting in the lowest localization error η_{opt}, an alternative strategy to optimize the radar subsystem is to minimize the total transmit power while satisfying the desired localization performance. Consider the maximum acceptable localization error η_{accept} such that $\eta_{\text{accept}} > \eta_{\text{opt}}$, the radar subsystem can minimize its power utilization as follows:

$$\begin{aligned} \min_{\mathbf{p}_{\text{tx}}} \quad & \mathbf{1}_M^{\text{T}} \mathbf{p}_{\text{tx}} \\ \text{subject to} \quad & \sigma^2_{x,y}(\mathbf{p}_{\text{tx}}) \leq \eta_{\text{accept}}, \\ & \mathbf{p}_{\text{tx,min}} \leq \mathbf{p}_{\text{tx}} \leq \mathbf{p}_{\text{tx,max}}, \end{aligned} \tag{20}$$

The optimization problem (20) is non-convex due to the constraint involving $\sigma^2_{x,y}(\mathbf{p}_{\text{tx}})$. We can first restrict this constraint to equality, i.e., $\sigma^2_{x,y}(\mathbf{p}_{\text{tx}}) = \eta_{\text{accept}}$. According to Eq. (13), this leads to the equality $\eta_{\text{accept}} \mathbf{p}_{\text{tx}}^{\text{T}} \mathbf{A} \mathbf{p}_{\text{tx}} - \mathbf{q}^{\text{T}} \mathbf{p}_{\text{tx}} = 0$. Accordingly, the problem (20) can be relaxed into the following convex form [38]:

$$\begin{aligned} \min_{\mathbf{p}_{\text{tx}}} \quad & \mathbf{1}_M^{\text{T}} \mathbf{p}_{\text{tx}} \\ \text{subject to} \quad & \mathbf{q} - \eta_{\text{accept}} \mathbf{A} \mathbf{p}_{\text{tx}} \leq \mathbf{0}, \\ & \mathbf{p}_{\text{tx,min}} \leq \mathbf{p}_{\text{tx}} \leq \mathbf{p}_{\text{tx,max}}. \end{aligned} \tag{21}$$

The solution to the relaxed convex optimization problem (21) yields the optimized transmit power that tends to achieve localization MSE less than η_{accept}.

B. Communication-only operation

Traditionally, communication systems maximize their performance by employing the maximum allowable power. For the case of maximizing the sum capacity, the optimal power allocation using the maximum allowable transmit power can be achieved by solving the following optimization problem:

$$\begin{aligned} \max_{\mathbf{p}_{\text{tx}}} \quad & \sum_{r=1}^{R} \sum_{m=1}^{M} \log \left(1 + \frac{p_{m,\text{tx}}}{\gamma_{m,r}} \right) \\ \text{subject to} \quad & \mathbf{p}_{\text{tx,min}} \leq \mathbf{p}_{\text{tx}} \leq \mathbf{p}_{\text{tx,max}}, \\ & \mathbf{1}_M^{\text{T}} \mathbf{p}_{\text{tx}} \leq P_{\text{total}_{\max}}. \end{aligned} \tag{22}$$

We can observe that each waveform is broadcast to all the communication receivers. This implies that the communication information transmitted to all the receivers is the same; however, the channel conditions are not necessarily the same for each communication receiver. Due to this fact, Shannon capacity for each individual receiver can be different depending on the channel conditions. The optimization problem (22) utilizes the maximum allowable power and distributes it to all the JRC transmitters based on the channel quality. In general, more power is allocated to the transmitters that have better overall channel conditions for the communication receivers. On the other hand, the transmitters having poor channel conditions are either largely ignored or allocated low power. Note that the communication receivers having good channel conditions benefit more under such a power allocation scheme. This can be undesirable for the communication receivers that have poor channel conditions but have critical importance. To fairly treat all users such that they are enabled with the same capacity, we can formulate the following worst-case optimization problem:

$$\begin{aligned} \max_{\mathbf{p}_{\text{tx}}} \min_{r} \quad & \sum_{m=1}^{M} \log\left(1+\frac{p_{m,\text{tx}}}{\gamma_{m,r}}\right) \\ \text{subject to} \quad & \mathbf{p}_{\text{tx,min}} \preceq \mathbf{p}_{\text{tx}} \preceq \mathbf{p}_{\text{tx,max}}, \\ & \mathbf{1}_M^{\mathrm{T}} \mathbf{p}_{\text{tx}} \leq P_{\text{total}_{\max}}. \end{aligned} \tag{23}$$

The above maximin optimization maximizes the worst-case capacity achieved by all communication receivers. Such approach tries to democratize the capacity distribution among the communication receivers rather than achieving the sum capacity maximization. This maximin problem is transformed for efficient solution by the gradient-based solvers, that require continuous first and second derivatives, allowing a rapid convergence to the solution. The maximin optimization problem (23) can be expressed in the following equivalent form:

$$\begin{aligned} \max_{\mathbf{p}_{\text{tx}}} \quad & z \\ \text{subject to} \quad & \sum_{m=1}^{M} \log\left(1+\frac{p_{m,\text{tx}}}{\gamma_{m,r}}\right) \geq z, \quad \forall r \\ & \mathbf{p}_{\text{tx,min}} \preceq \mathbf{p}_{\text{tx}} \preceq \mathbf{p}_{\text{tx,max}}, \\ & \mathbf{1}_M^{\mathrm{T}} \mathbf{p}_{\text{tx}} \leq P_{\text{total}_{\max}}, \end{aligned} \tag{24}$$

where z is an auxiliary variable representing the minimum capacity achieved by all the communication users.

Depending on the communication objectives, either sum communication capacity or worst-case communication capacity can be used to evaluate the performance of overall communication system. Sum communication capacity is important when superior communication performance is desired for the communication receivers with better channel conditions. On the other hand, worst-case communication capacity is important when each communication receiver must receive the same communication capacity regardless of their channel conditions.

V. Cooperative Power Allocation for Distributed MIMO JRC

The optimal power allocation schemes expressed in Section IV are designed for either radar-only or communication-only operation. The resulting power allocation from these schemes do not account for both radar and communication channel conditions simultaneously and, therefore, are not optimized for cooperative JRC system operations. In this section, we develop cooperative resource allocation strategies for the JRC system that simultaneously optimize both radar and communication objectives. In this context, we consider radar as the primary function of the JRC system, whereas the communication operation is the secondary objective.

We present two resource allocation schemes for the JRC system, as illustrated in Fig. 3. The first scheme uses a shared approach where the waveforms transmitted by the dual-purpose JRC transmitters are exploited by both radar and communication systems. This is evident in Fig. 3(a) where only one waveform is transmitted from the JRC transmit antenna. Such strategy is useful when a limited number of

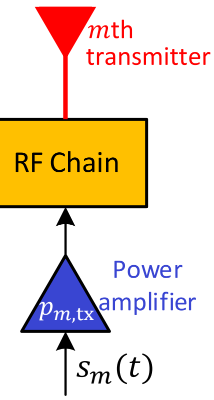

(a) Transmission of shared waveform for radar and communication tasks

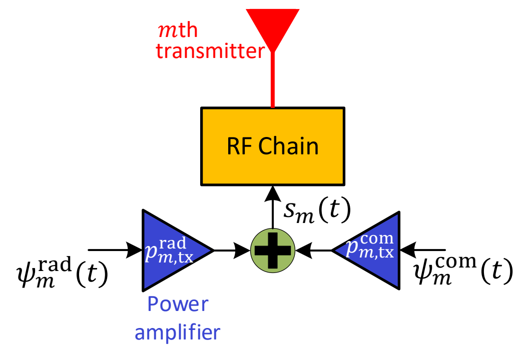

(b) Joint transmission of two waveforms respectively dedicated for radar and communication tasks

Fig. 3: Transmission strategy at mth transmit antenna ($m = 1, \cdots, M$) for distributed MIMO JRC system using shared and dedicated waveforms.

orthogonal waveforms are available. In the second scheme, the communication and radar subsystems exploit different sets of waveforms that are respectively dedicated to these two subsystems without sharing the waveforms. This approach is more flexible in the sense that the JRC system can change the radar waveforms depending on the radar channel conditions and the nature of target surveillance. This scheme is depicted in Fig. 3(b) where dedicated communication and radar waveforms are transmitted from a single RF transmit chain. It is observed that the transmit waveform emitted from each antenna is the sum of two waveforms respectively dedicated for the radar and the communication tasks.

A. Power allocation using the shared waveforms

In this resource allocation strategy, we assume that the radar and communication subsystems exploit the same waveforms simultaneously. The JRC system first employs the radar-centric optimization problem (19) to achieve the best localization MSE η_{opt} that can be achieved for the radar task. Subsequently, the JRC system decides the error flexibility parameter $\gamma_{\text{flex}} = \eta_{\text{flex}}/\eta_{\text{opt}}$ $(0 \leq \gamma_{\text{flex}} \leq 1)$. Note that η_{opt} is obtained using optimization problem (19) that provides the best target localization performance, whereas $\eta_{\text{flex}} \geq \eta_{\text{opt}}$ is the flexible localization error specified for the JRC system in the cooperative scheme. A higher value of γ_{flex} favors the radar objective, whereas a lower value provides a higher flexibility to optimize the communication function at the cost of reduced target localization accuracy. In particular, when $\gamma_{\text{flex}} = 1$, η_{flex} will be equal to η_{opt}, implying that the communication objective is ignored and the overall precedence of the JRC system will be to minimize the target localization error. On the other hand, when $\gamma_{\text{flex}} = 0$, η_{flex} becomes zero and the sole precedence of the JRC system is given to the communication objectives. Generally, the JRC system is provided with the worst-case acceptable target localization error in terms of η_{flex}.

We incorporate the communication objectives and total power constraint in the optimization problem (21) to simultaneously satisfy both radar and communication objectives. This results in the following optimization problem that maximizes the sum capacity of the communication subsystem while achieving localization MSE η_{flex} for the radar subsystem:

$$\begin{aligned} \max_{\mathbf{p}_{\text{tx}}} \quad & \sum_{n=1}^{N}\sum_{m=1}^{M} \log\left(1+\frac{p_{m,\text{tx}}}{\gamma_{m,r}}\right) \\ \text{subject to} \quad & \mathbf{q} - \eta_{\text{flex}}\mathbf{A}\mathbf{p}_{\text{tx}} \leq \mathbf{0}, \\ & \mathbf{p}_{\text{tx,min}} \leq \mathbf{p}_{\text{tx}} \leq \mathbf{p}_{\text{tx,max}}, \\ & \mathbf{1}_M^{\text{T}}\mathbf{p}_{\text{tx}} \leq P_{\text{total}_{\text{max}}}. \end{aligned} \tag{25}$$

Similarly, when the worst-case communication capacity is used as the criterion, the optimization problem becomes

$$\begin{aligned} \max_{\mathbf{p}_{\text{tx}}}\ \min_{r} \quad & \sum_{m=1}^{M} \log\left(1+\frac{p_{m,\text{tx}}}{\gamma_{m,r}}\right) \\ \text{subject to} \quad & \mathbf{q} - \eta_{\text{flex}}\mathbf{A}\mathbf{p}_{\text{tx}} \leq \mathbf{0}, \\ & \mathbf{p}_{\text{tx,min}} \leq \mathbf{p}_{\text{tx}} \leq \mathbf{p}_{\text{tx,max}}, \\ & \mathbf{1}_M^{\text{T}}\mathbf{p}_{\text{tx}} \leq P_{\text{total}_{\text{max}}}. \end{aligned} \tag{26}$$

The optimization problems (25) and (26) provide optimal power allocation for distributed JRC transmitters under the maximum allowable power constraint such that the localization MSE for the radar operation is bounded by η_{flex}. At the same time, the objective functions optimize the performance of communication system by maximizing sum communication capacity or worst-case communication capacity, respectively. Note that the optimized power $p_{m_{\text{tx}}}^{\text{opt}}, \forall m$ achieved by the optimization problems (25) and (26) illustrates the respective power for the transmit waveforms $s_m(t)$ that are shared by both radar and communication systems. Since all the base waveforms are known at the communication receivers for the purpose of information transfer, this system does not allow the flexibility of real-time radar waveform design depending on the radar channel conditions and the nature of target.

B. Power allocation using the dedicated waveforms

In this resource allocation strategy, the radar and communication subsystems exploit different waveforms. These waveforms are designed to be orthogonal so that no interference between them is considered. The use of separate waveforms allows the JRC system to change the radar waveforms depending on the radar channel conditions and the nature of the target, independent of the communication requirements and conditions. In other words, this flexibility of changing radar waveforms does not affect the communication subsystem operation because the communication users exploit their dedicated set of waveforms which are orthogonal to the radar waveforms.

Let $\mathbf{\Psi}_{\text{rad}}$ and $\mathbf{\Psi}_{\text{com}}$ be the mutually exclusive sets, respectively representing the dictionaries of radar and communication waveforms, such that $\mathbf{\Psi}_{\text{rad}}$ and $\mathbf{\Psi}_{\text{com}}$ are subsets of $\mathbf{\Psi}$. All the waveforms in the dictionary set $\mathbf{\Psi}$ are assumed to be orthogonal to each other. The transmit waveform from the mth JRC transmitter is expressed as the combination of radar waveform $\psi_m^{\text{rad}}(t)$ and communication waveform $\psi_m^{\text{com}}(t)$, i.e.,

$$s_m(t) = \psi_m^{\text{rad}}(t) + \psi_m^{\text{com}}(t), \tag{27}$$

where $\psi_m^{\text{rad}}(t) \in \mathbf{\Psi}_{\text{rad}}$ and $\psi_m^{\text{com}}(t) \in \mathbf{\Psi}_{\text{com}}$.

Although this scheme is challenging in the sense that it is difficult to extract a high number of orthogonal waveforms, this strategy offers high flexibility in real-time radar waveform design.

Consider two power vectors $\mathbf{p}_{\text{tx}}^{\text{rad}}$ and $\mathbf{p}_{\text{tx}}^{\text{com}}$ which respectively represent the transmit powers for the radar and communication waveforms from the JRC system, i.e.,

$$\begin{aligned} \mathbf{p}_{\text{tx}}^{\text{rad}} &= [p_{1_{\text{tx}}}^{\text{rad}}, p_{2_{\text{tx}}}^{\text{rad}}, \ldots, p_{M_{\text{tx}}}^{\text{rad}}]^{\text{T}}, \\ \mathbf{p}_{\text{tx}}^{\text{com}} &= [p_{1_{\text{tx}}}^{\text{com}}, p_{2_{\text{tx}}}^{\text{com}}, \ldots, p_{M_{\text{tx}}}^{\text{com}}]^{\text{T}}, \end{aligned} \tag{28}$$

where $p_{m_{\text{tx}}}^{\text{rad}}$ and $p_{m_{\text{tx}}}^{\text{com}}$ respectively represent the powers allocated to waveforms $\psi_m^{\text{rad}}(t)$ and $\psi_m^{\text{com}}(t)$, and $\mathbf{p}_{\text{tx}} = \mathbf{p}_{\text{tx}}^{\text{rad}} + \mathbf{p}_{\text{tx}}^{\text{com}}$ denotes the total power transmitted for both radar and communication waveforms.

The JRC system first determines the optimal localization MSE η_{opt} by employing the radar-centric optimization problem (19) and decides its flexibility parameter γ_{flex} that leads to the localization MSE $\eta_{\text{flex}} = \eta_{\text{opt}}/\gamma_{\text{flex}}$. Subsequently, the optimization problem (21) is modified to incorporate the communication objectives and the total power constraint, resulting in the following cooperative power allocation strategy that maximizes the sum communication capacity while achieving the target localization MSE less than η_{flex}:

$$\begin{aligned} \max_{\mathbf{p}_{\text{tx}}^{\text{rad}}, \mathbf{p}_{\text{tx}}^{\text{com}}} \quad & \sum_{n=1}^{N}\sum_{m=1}^{M} \log\left(1+\frac{p_{m,\text{tx}}^{\text{com}}}{\gamma_{m,r}}\right) \\ \text{subject to} \quad & \mathbf{q} - \eta_{\text{flex}}\mathbf{A}\mathbf{p}_{\text{tx}}^{\text{rad}} \leq \mathbf{0}, \\ & \mathbf{p}_{\text{tx,min}} \leq \mathbf{p}_{\text{tx}}^{\text{rad}} + \mathbf{p}_{\text{tx}}^{\text{com}} \leq \mathbf{p}_{\text{tx,max}}, \\ & \mathbf{1}_M^{\text{T}}(\mathbf{p}_{\text{tx}}^{\text{rad}} + \mathbf{p}_{\text{tx}}^{\text{com}}) \leq P_{\text{total}_{\text{max}}}. \end{aligned} \tag{29}$$

Similarly, we can formulate the worst-case optimization problem that maximizes the minimum Shannon capacity achieved by all the communication users as:

$$\begin{aligned} \max_{\mathbf{p}_{\text{tx}}^{\text{rad}}, \mathbf{p}_{\text{tx}}^{\text{com}}}\ \min_{r} \quad & \sum_{m=1}^{M} \log\left(1+\frac{p_{m,\text{tx}}^{\text{com}}}{\gamma_{m,r}}\right) \\ \text{subject to} \quad & \mathbf{q} - \eta_{\text{flex}}\mathbf{A}\mathbf{p}_{\text{tx}}^{\text{rad}} \leq \mathbf{0}, \\ & \mathbf{p}_{\text{tx,min}} \leq \mathbf{p}_{\text{tx}}^{\text{rad}} + \mathbf{p}_{\text{tx}}^{\text{com}} \leq \mathbf{p}_{\text{tx,max}}, \\ & \mathbf{1}_M^{\text{T}}(\mathbf{p}_{\text{tx}}^{\text{rad}} + \mathbf{p}_{\text{tx}}^{\text{com}}) \leq P_{\text{total}_{\text{max}}}. \end{aligned} \tag{30}$$

The use of dedicated waveforms for radar and communication tasks requires the JRC system be equipped with a high number of orthogonal waveforms; however, this strategy also provides flexibility to the JRC system allowing real-time radar waveform design. Moreover, the dedicated radar and communication waveform scheme will split the power between the two functions, rendering lower overall performance compared to the case when the waveforms are shared by both subsystems.

VI. Extension to Multiple Target Scenario

In this section, we discuss the extension of the proposed power allocation schemes for multiple-target scenarios. Assume that the ith target is located at the coordinate (x_i, y_i), where $i = 1, \cdots, I$ represents the target index, and I is the total number of targets. Using the RCS and channel information $\mathbf{h}_i, \forall i$ and the estimated target locations, we can readily calculate the parameters $\mathbf{q}_i$ and $\mathbf{A}_i$ for each target by exploiting Eq. (14) in the same manner as done for the single target case. The following formulations can be employed for the JRC power optimization problems in the presence of multiple targets.

Similar to problem (25), localization MSE of $\eta_{i,\text{achieve}}$ can be achieved for the ith target, $\forall i = 1, \cdots, I$, while maximizing the communication throughput using the shared waveforms as follows:

$$\begin{aligned} \max_{\mathbf{p}_{\text{tx}}} \quad & \sum_{n=1}^{N}\sum_{m=1}^{M} \log\left(1+\frac{p_{m,\text{tx}}}{\gamma_{m,r}}\right) \\ \text{subject to} \quad & \mathbf{q}_i - \eta_{i,\text{achieve}}\mathbf{A}_i\mathbf{p}_{\text{tx}} \leq \mathbf{0}, \quad i=1,\cdots,I, \\ & \mathbf{p}_{\text{tx,min}} \leq \mathbf{p}_{\text{tx}} \leq \mathbf{p}_{\text{tx,max}}, \\ & \mathbf{1}_M^{\mathrm{T}}\mathbf{p}_{\text{tx}} \leq P_{\text{total}_{\max}}. \end{aligned} \tag{31}$$

Similarly, the power optimization problem (26) for maximizing the worst-case communication capacity can be modified as follows:

$$\begin{aligned} \max_{\mathbf{p}_{\text{tx}}} \min_{r} \quad & \sum_{m=1}^{M} \log\left(1+\frac{p_{m,\text{tx}}}{\gamma_{m,r}}\right) \\ \text{subject to} \quad & \mathbf{q}_i - \eta_{i,\text{achieve}}\mathbf{A}_i\mathbf{p}_{\text{tx}} \leq \mathbf{0}, \quad i=1,\cdots,I, \\ & \mathbf{p}_{\text{tx,min}} \leq \mathbf{p}_{\text{tx}} \leq \mathbf{p}_{\text{tx,max}}, \\ & \mathbf{1}_M^{\mathrm{T}}\mathbf{p}_{\text{tx}} \leq P_{\text{total}_{\max}}. \end{aligned} \tag{32}$$

For the JRC MIMO system exploiting the dedicated waveforms respectively for radar and communication subsystems, the problem (29) for maximizing the communication capacity can be formulated for the multiple target case as follows:

$$\begin{aligned} \max_{\mathbf{p}_{\text{tx}}^{\text{rad}},\mathbf{p}_{\text{tx}}^{\text{com}}} \quad & \sum_{n=1}^{N}\sum_{m=1}^{M} \log\left(1+\frac{p_{m,\text{tx}}^{\text{com}}}{\gamma_{m,r}}\right) \\ \text{subject to} \quad & \mathbf{q}_i - \eta_{i,\text{achieve}}\mathbf{A}_i\mathbf{p}_{\text{tx}}^{\text{rad}} \leq \mathbf{0}, \quad i=1,\cdots,I, \\ & \mathbf{p}_{\text{tx,min}} \leq \mathbf{p}_{\text{tx}}^{\text{rad}} + \mathbf{p}_{\text{tx}}^{\text{com}} \leq \mathbf{p}_{\text{tx,max}}, \\ & \mathbf{1}_M^{\mathrm{T}}(\mathbf{p}_{\text{tx}}^{\text{rad}} + \mathbf{p}_{\text{tx}}^{\text{com}}) \leq P_{\text{total}_{\max}}. \end{aligned} \tag{33}$$

Similarly, the power optimization problem (30) for maximizing the worst-case communication capacity using dedicated radar and communication waveforms can be modified as follows:

$$\begin{aligned} \max_{\mathbf{p}_{\text{tx}}^{\text{rad}},\mathbf{p}_{\text{tx}}^{\text{com}}} \min_{r} \quad & \sum_{m=1}^{M} \log\left(1+\frac{p_{m,\text{tx}}^{\text{com}}}{\gamma_{m,r}}\right) \\ \text{subject to} \quad & \mathbf{q}_i - \eta_{i,\text{achieve}}\mathbf{A}_i\mathbf{p}_{\text{tx}}^{\text{rad}} \leq \mathbf{0}, \quad i=1,\cdots,I, \\ & \mathbf{p}_{\text{tx,min}} \leq \mathbf{p}_{\text{tx}}^{\text{rad}} + \mathbf{p}_{\text{tx}}^{\text{com}} \leq \mathbf{p}_{\text{tx,max}}, \\ & \mathbf{1}_M^{\mathrm{T}}(\mathbf{p}_{\text{tx}}^{\text{rad}} + \mathbf{p}_{\text{tx}}^{\text{com}}) \leq P_{\text{total}_{\max}}. \end{aligned} \tag{34}$$

Ensuring the radar constraints in problems (31)–(34) can sometimes lead to challenging situations. For example, if the RCS and the channel gains of one target are too low compared to the other targets, the JRC system will tend to give higher precedence to the weaker target in order to improve its localization performance, especially if the required localization accuracy is the same for all the targets. This can lead to poor localization performance for other targets even when they have a large RCS and good channel conditions. In such situations, it becomes important to intelligently select different $\eta_{i,\text{achieve}}$ for different targets depending on their RCS and channel gains. It should also be noted that these approaches may not always have a feasible solution if the desired MSE $\eta_{i,\text{achieve}}$ cannot be achieved for a subset of targets due to the varying channel conditions and the constraints on the available power.

VII. Information Embedding

Information embedding can be accomplished in several ways. Inspired by the waveform diversity scheme [12] and phase modulation scheme [15], we provide two simple information embedding schemes for the distributed MIMO JRC system as follows.

Let $\boldsymbol{\varphi}_m(t) = [\varphi_{m,1}(t), \cdots, \varphi_{m,K}(t)]^{\mathrm{T}}$ represent the waveform dictionary matrix of K orthogonal waveforms available to the mth transmitter. The mth transmitter employs an $K \times 1$ information vector $\mathbf{b}_m$, for $m = 1, \cdots, M$, representing the information to be transmitted by the transmitter. The waveform transmitted from the mth transmitter during a radar pulse is given as

$$s_m(t) = \mathbf{b}_m^{\mathrm{T}}\boldsymbol{\varphi}_m(t). \tag{35}$$

The signal transmitted by the mth transmitter and received at the communication receiver r is given by

$$s_{m,r}^{\text{com}}(t) = \sqrt{\beta_{m,r}p_{m_{\text{tx}}}}g_{m,r}s_m(t-\kappa_{m,r}) + w_{m,r}^{\text{com}}(t). \tag{36}$$

Matched filtering at the rth communication receiver using the kth orthogonal waveform results in the following output

$$y_{r,m,k} = \begin{cases} e^{j\theta_{m,r,k}}\tilde{g}_{m,r} + w_{r,m,k}, & \text{if } \varphi_{m,k}(t) \text{ transmitted}, \\ w_{r,m,k}, & \text{otherwise}, \end{cases} \tag{37}$$

where $e^{j\theta_{m,r,k}}$ is the received initial phase of the transmit waveform $\varphi_{m,k}(k)$ at the rth receiver, $\tilde{g}_{m,r} = \sqrt{\beta_{m,r}p_{m_{\text{tx}}}}g_{m,r}$ is the received signal amplitude, and $w_{r,m,k}$ is the noise term.

A. Waveform Diversity

In this scheme, communication information is embedded by each transmitter in the form of waveform selection. During each radar pulse, the mth transmitter selects $\bar{K}_m$ waveforms ($\bar{K}_m \leq K$) from its dictionary of available waveforms. The transmit information in this case is represented by the vector $\mathbf{b}_m$ such that $\mathbf{1}^{\mathrm{T}}\mathbf{b}_m = \bar{K}_m$ for $m = 1, \cdots, M$. The communication receivers apply match filter on the receiver signal to estimate which set of waveforms is transmitted by the JRC transmitters. An example of a simple scenario for this case is when $K = 2$ and $\bar{K}_m = 1$.

B. Phase Modulation

In this scheme, communication information is embedded in the form of the initial phase of transmit waveforms at each transmitter. Each transmitter transmits K orthogonal waveforms such that $\varphi_{m,1}(t)$ denotes the reference waveform. The K elements of information vector $\mathbf{b}_m$, for $m = 1, \cdots, M$, are complex exponentials representing the initial phases of respective waveforms transmitted by the transmitter. In other words, the element $b_{m,k}$, representing the kth element of $\mathbf{b}_m$, is the transmit initial phase for $\varphi_{m,k}(t)$. Each communication receiver performs matched filtering and extracts the $K-1$ phase symbols by employing $\angle(b_{m,1}/b_{m,k}) = \theta_k$, where $k = 2, \cdots, K$. In this context, the simplest information embedding scenario occurs when $K = 2$.

Orthogonal waveform design is a challenging task in MIMO radar [46]. As we can see from the above two information embedding schemes, a total of KM orthogonal waveforms are required for the distributed JRC system. For a large number of transmitters, such a requirement can be difficult to satisfy. This difficulty should be kept under consideration while designing the JRC system.

Note that the Shannon capacity used to optimize communication system performance is a theoretical limit that cannot be achieved in practice. There is typically a large gap between the actual performance and capacity. However, this does not mean that Shannon capacity is not useful. Irrespective of the information embedding scheme, increasing Shannon capacity generally results in improved communication system performance either in the form of enhanced data rate or reduced probability of error [47, 48]. The achieved data rate tends to approach Shannon capacity as the information embedding scheme becomes more sophisticated [48].

VIII. Simulation Results

In this section, we investigate the performance of the proposed JRC techniques using computer simulations. All optimization problems were solved using CVX toolbox [49].

Consider a distributed JRC MIMO system consisting of $M = 5$ isotropic transmitters located at $(550, 600)$ m, $(291, 961)$ m, $(18, 440)$ m, $(428, 20)$ m, and $(955, 280)$ m, respectively, in the 2-D space. The distributed MIMO radar uses $N = 5$ receive antennas located at $(900, 553)$ m, $(628, 975)$ m, $(85, 773)$ m, $(133, 187)$ m, and $(705, 51)$ m, respectively. Two communication receivers are located at $(50, 375)$ m and $(375, 60)$ m, respectively. Each transmitter can transmit a maximum of 100 W power during each radar pulse, whereas the maximum total allowable transmit power, $P_{\mathrm{total}_{\max}}$, is 300 W. Moreover, the carrier frequency is assumed to be 6 GHz, and the parameter $\xi_m = 1.83 \times 10^4 \mathrm{W}^{-1}\mathrm{m}^{-2}, \forall m$ is considered. Fig. 4 shows the arrangement of the distributed JRC MIMO in the 2-D coordinate system.

The path loss coefficients $\beta_{m,r}$ for the communication subsystem can be calculated using the relative location coordinates of the distributed JRC MIMO system and the communication receivers. The communication SNR is given as follows:

$$\mathbf{\Lambda} = \begin{pmatrix} 0.0018 & 0.0018 \\ 0.7886 & 0.9467 \\ 12.9519 & 0.0040 \\ 1.2359 & 10.6520 \\ 0.5714 & 1.1375 \end{pmatrix}, \tag{38}$$

where the (m,r)th element of $\mathbf{\Lambda}$ is given as $[\mathbf{\Lambda}]_{m,r} = \beta_{m,r}|g_{m,r}|^2/\sigma^2_{m,r}$ For the sake of simplicity, we assume waveform diversity scheme with $\bar{K}_m = 1$ and $K = 2$.

A. Single Target Case:

First, we consider a point target located at $(500, 500)$ m as shown in Fig. 4. The magnitudes and phases of all elements of the RCS vector $\mathbf{h}$ are assumed to follow Gaussian distribution. The path loss coefficients $\alpha_{m,n}$ for the target are computed using the relative distance of target w.r.t. the distributed JRC MIMO system. For the convenience of reproduction of the simulation results, we provide the propagation gains resulting from the setup in Fig. 4 as follows:

$$\mathbf{\Upsilon} = \begin{pmatrix} 38.52 & 1.76 & 103.32 & 1.57 & 7.74 \\ 2.10 & 0.10 & 6.19 & 0.09 & 0.44 \\ 0.40 & 0.02 & 1.18 & 0.02 & 0.08 \\ 18.09 & 0.83 & 53.67 & 0.76 & 3.53 \\ 0.44 & 0.02 & 1.33 & 0.02 & 0.09 \end{pmatrix} \times 10^{-9}, \tag{39}$$

where the (m,n)th element of $\mathbf{\Upsilon}$ is given as $[\mathbf{\Upsilon}]_{m,n} = \sqrt{\alpha_{m,n}} h_{m,n}$.

1) Radar- and Communication-centric Design: From the simulation setting, it can be observed that the first transmitter has overall the best channel conditions for the radar subsystem and the worst channel conditions for the communication

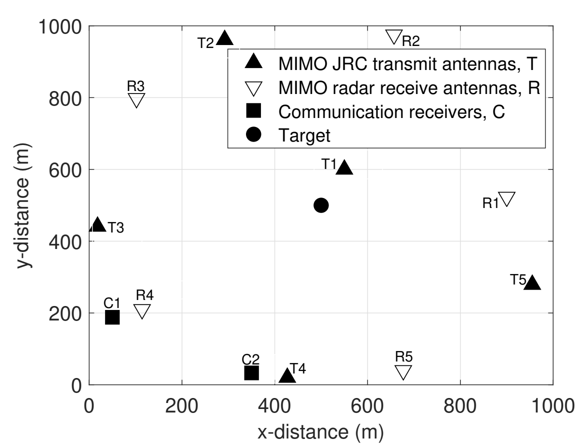

Fig. 4: Simulation layout for distributed JRC MIMO system.

TABLE I: Optimized power allocation for individual radar and communication systems

	Radar-centric (19)	Communication--centric max. sum capacity (22)	Communication--centric worst-case (23)
$\mathbf{p}_{\text{tx}}$ (W)	$\begin{bmatrix}100\\100\\0\\100\\0\end{bmatrix}$	$\begin{bmatrix}0\\83.44\\49.14\\84.12\\83.3\end{bmatrix}$	$\begin{bmatrix}0\\99.17\\1.5\\100\\99.33\end{bmatrix}$
P_{total} (W)	300	300	300
$\sqrt{\eta}$ (m)	$\sqrt{\eta_{\text{opt}}} = 2.24$	4.60	4.25
$\Re$ (bits/sec/Hz)	30.39	50.66	46.93

TABLE II: Cooperative power allocation for JRC system using shared waveforms

	Cooperative max. sum capacity (25)	Cooperative worst-case (26)
$\mathbf{p}_{\text{tx}}$ (W)	$\begin{bmatrix}99.43\\56.06\\29.90\\61.75\\52.86\end{bmatrix}$	$\begin{bmatrix}97.34\\65.96\\1.47\\72.62\\62.61\end{bmatrix}$
P_{total} (W)	300	300
$\sqrt{\eta_{\text{flex}}}$ (m)	2.39	2.39
$\Re$ (bits/sec/Hz)	47.02	43.98

subsystem. This implies that the first transmitter plays the most important role in localizing the target; however, it has the least importance for achieving high communication capacity due to the poor communication channels with both communication receivers. It is also observed that the third transmitter has poor channel conditions with the second communication receiver, even though it has a very high channel gain for the first communication receiver.

Table I shows the optimized power allocation profile for radar- and communication-centric operations. For the radar-centric case, it is observed that most of the transmit power is allocated to the transmitters that have good radar channel conditions to obtain the lowest mean localization error $\sqrt{\eta_{\text{opt}}} = 2.24$ m. The signals using such power allocation, when used for communication purpose, result in a low sum Shannon capacity of 30.39 bits/sec/Hz. On the other hand, the communication-centric optimization that maximizes the sum Shannon capacity allocates most of the power to the transmitters with favorable communication channels. Contrary to that, communication-centric operation maximizing the worst-case communication capacity allocates most power in the channels that are equally good for both communication receivers so as to achieve the same Shannon capacity for both communication receivers. This is evidently demonstrated in this example that, even though the third transmitter had the best channel conditions for the first communication receiver, least power is allocated to it due to its poor channel conditions with the second communication receiver. Moreover, all the communication-centric approaches result in a very high localization error for the radar subsystem.

2) Joint Radar-Communications: Now we perform cooperative power allocation for the JRC system by keeping the mean localization error $\sqrt{\eta_{\text{flex}}} = 2.39$ m for all the simulations unless otherwise specified. Table II shows the results for cooperative JRC power allocation by exploiting shared waveforms. It is observed that, contrary to radar- and communication-centric designs, the cooperative design achieves good performance for both radar and communication subsystems. It is evident that the cooperative design proportionally allocates more power to the transmitters that are good for both radar and communication tasks so as to achieve the objectives of both subsystems. Fig. 5 shows the performance of the cooperative JRC power allocation strategy that trades off between the radar target localization error and the communication Shannon capacity. The left and right edges of all the curves respectively correspond to radar- and communication-centric operations. The curves discontinue on

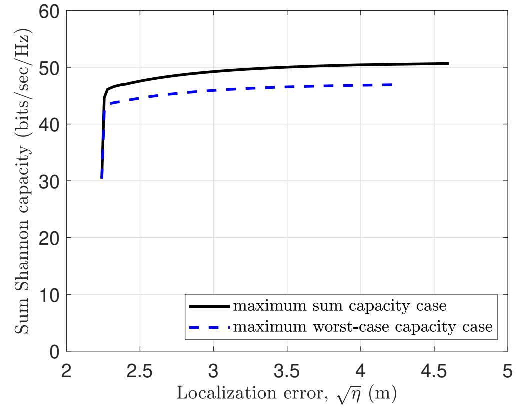

(a) Sum communication capacities vs. target localization error

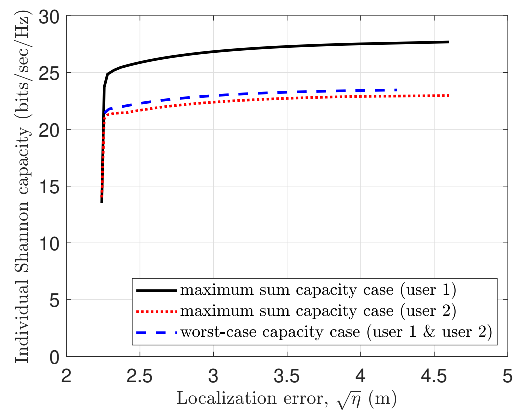

(b) Individual communication capacities vs. target localization error

Fig. 5: Communication capacities versus radar target localization error for JRC power allocation schemes exploiting shared waveforms for radar and communication functions.

TABLE III: Cooperative power allocation for JRC system using dedicated waveforms and sum capacity optimization (29)

	Radar-only	Communication-only	Overall
Transmit powers (W)	$\mathbf{p}_{\text{tx}}^{\text{rad}} = \begin{bmatrix}100\\0\\0\\81.76\\0\end{bmatrix}$	$\mathbf{p}_{\text{tx}}^{\text{com}} = \begin{bmatrix}0\\39.21\\21.72\\18.24\\39.07\end{bmatrix}$	$\mathbf{p}_{\text{tx}} = \begin{bmatrix}100\\39.21\\21.72\\100\\39.07\end{bmatrix}$
Total Power (W)	181.76	118.24	300
$\sqrt{\eta_{\text{flex}}}$ (m)	2.39	–	2.39
$\Re$ (bits/sec/Hz)	–	40.72	40.72

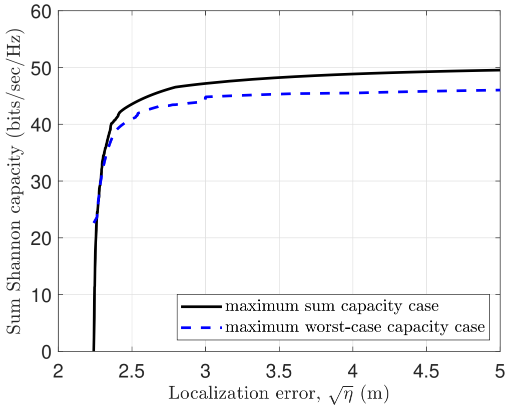

(a) Sum communication capacities vs. target localization error

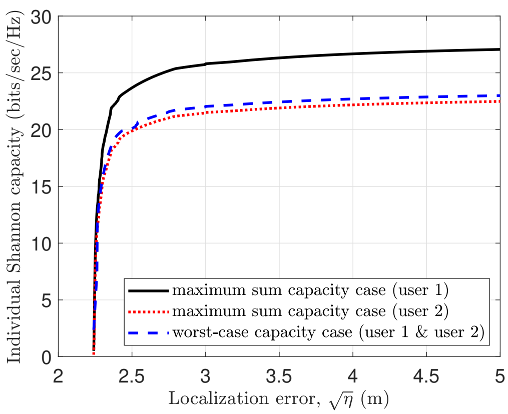

(b) Individual communication capacities vs. target localization error

Fig. 6: Communication capacities versus radar target localization error for JRC power allocation schemes exploiting dedicated waveforms for radar and communication functions.

the right-hand side as the resulting power allocations at those communication-centric points reach the worst-possible radar localization error that could be achieved while using all the available power.

Tables III and IV respectively show the results of the cooperative JRC power allocation strategies exploiting dedicated waveforms for sum and worst-case Shannon capacity maximization. It is observed that most power for radar- and communication-dedicated waveforms is proportionally allocated to the channels that have respectively good conditions. Moreover, the worst-case Shannon capacity maximization maximizes the minimum achieved capacity by the communication receivers by allocating transmit power to the transmitters that have equally good channel conditions for both receivers. Since the total power is split between radar and communication waveforms for these schemes, the resulting communication capacity is lower than the capacity achieved by the JRC system exploiting shared waveforms for the same target localization error.

Fig. 6 shows the performance of cooperative JRC power allocation using dedicated waveforms with varying radar and communication performance. The left and right edges of all the curves respectively show the radar- and communication-centric operation. In this case, the communication capacity for radar-centric designs is 0, unlike Fig. 5, because all the power is dedicated to radar waveforms to minimize the target location error. Also note that all the curves do not have an edge on the right-hand side because if all the power is allocated to the communication-dedicated waveforms, the radar system will have an infinite localization error as no power is allocated for radar operation.

TABLE IV: COOPERATIVE POWER ALLOCATION FOR JRC SYSTEM USING DEDICATED WAVEFORMS AND WORST-CASE CAPACITY OPTIMIZATION (30)

	Radar-only	Communication Only	Overall
Transmit powers (W)	$\mathbf{p}_{\text{tx}}^{\text{rad}} = \begin{bmatrix} 100 \\ 4.15 \\ 0 \\ 80.04 \\ 0 \end{bmatrix}$	$\mathbf{p}_{\text{tx}}^{\text{com}} = \begin{bmatrix} 0 \\ 47.13 \\ 1.43 \\ 19.96 \\ 47.29 \end{bmatrix}$	$\mathbf{p}_{\text{tx}} = \begin{bmatrix} 100 \\ 51.28 \\ 1.43 \\ 100 \\ 47.29 \end{bmatrix}$
Total Power (W)	184.19	115.81	300
$\sqrt{\eta_{\text{flex}}}$ (m)	2.39	–	2.39
$\Re$ (bits/sec/Hz)	–	38.07	38.07

B. Multiple Target Case:

Consider a second target appearing at (50, 250) m which is assumed to have the same RCS as the first target. Moreover, the path loss coefficients of the second target can also be calculated using its coarsely estimated location and the location coordinates of the distributed JRC MIMO system. For multiple target simulations, we desire all the targets to achieve a localization MSE less than $\eta_{i,\text{achieve}} \leq 10$ m^2. Tables V and VII show the achieved localization errors of the two targets after solving their respective optimization problems.

Table V shows the results for cooperative JRC power allocation by exploiting shared waveforms obtained from problems (31) and (32). It is observed that the cooperative design proportionally allocates more power to the transmitters that have high gains towards both radar and communication tasks in order to achieve the objectives of both subsystems. Compared to the results depicted in Table II for the single-target case, it is observed that more power is now allocated to transmitter 3 because of the proximity of the second target with the transmitter 3, resulting in a reduced propagation loss. Therefore, the optimization problems (31) and (32) prioritize transmitter 3 accordingly while achieving similar localization errors and communication capacities as those obtained in the single-target case. For a single-target case, it can be observed from Table II that the transmitter 1 was allocated most of the power due to its proximity with the first target. When the second target is added in the scenario, Table V shows more precedence given to transmitter 3 due to its proximity and

TABLE V: MULTI-TARGET COOPERATIVE POWER ALLOCATION FOR JRC SYSTEM USING SHARED WAVEFORMS

	Cooperative max. sum capacity (31)	Cooperative worst-case (32)
$\mathbf{p}_{\text{tx}}$ (W)	$\begin{bmatrix} 67.36 \\ 42.75 \\ 90.95 \\ 56.8 \\ 42.13 \end{bmatrix}$	$\begin{bmatrix} 67.49 \\ 43.56 \\ 91.15 \\ 55.51 \\ 42.26 \end{bmatrix}$
P_{total} (W)	300	300
$\sqrt{\eta_{1,\text{achieve}}}$ (m)	2.79	2.80
$\sqrt{\eta_{2,\text{achieve}}}$ (m)	2.82	2.82
$\Re$ (bits/sec/Hz)	47.13	47.12

TABLE VI: MULTI-TARGET COOPERATIVE POWER ALLOCATION FOR JRC SYSTEM USING DEDICATED WAVEFORMS AND SUM CAPACITY OPTIMIZATION (33)

	Radar-only	Communication-only	Overall
Transmit powers (W)	$\mathbf{p}_{\rm tx}^{\rm rad} = \begin{bmatrix} 77.45 \\ 0 \\ 96.86 \\ 3.72 \\ 0 \end{bmatrix}$	$\mathbf{p}_{\rm tx}^{\rm com} = \begin{bmatrix} 0 \\ 39.42 \\ 3.13 \\ 40.13 \\ 39.28 \end{bmatrix}$	$\mathbf{p}_{\rm tx} = \begin{bmatrix} 77.45 \\ 39.42 \\ 100 \\ 43.86 \\ 39.28 \end{bmatrix}$
Total Power (W)	178.03	121.96	300
$\sqrt{\eta_{1,\rm achieve}}$ (m)	3.09	–	3.09
$\sqrt{\eta_{2,\rm achieve}}$ (m)	3.05	–	3.05
$\Re$ (bits/sec/Hz)	–	40.13	40.13

better channel conditions with the second target. Meanwhile, the power allocated to transmitter 1 is still reasonable.

Tables VI and VII respectively show the results of the cooperative JRC power allocation strategies exploiting dedicated waveforms for sum and worst-case Shannon capacity optimization problems. It is observed that most power for radar- and communication-dedicated waveforms is allocated to the channels that have better conditions for the respective subsystems. Contrary to the single-target results depicted in Table III, transmitter 3 is now allocated with more radar-centric power because of its proximity to the second target. Moreover, the total power shown in Tables VI and VII is split between radar and communication tasks, so the resulting communication capacity is lower than that achieved by the JRC system exploiting shared waveforms, as depicted in Table V.

Note that the desired target localization error in all the multiple target simulations is less than $\sqrt{\eta_{i,\rm achieve}} = 3.16$ m. Since the radar function is the primary operation of the JRC system, more precedence is given to satisfy the target localization performance metrics, described as radar constraints in problems (31)–(34). We also observe that the localization as well as the communication performance is better when a shared waveform is used instead of dedicated waveforms. This is because all available power can be used for both radar and communication purposes when shared waveform is used, resulting in better localization accuracy and communication throughput.

Simulation results illustrate that the optimized JRC systems achieve better performance for the joint operation of radar and communication subsystems compared to radar- and communication-centric designs.

TABLE VII: MULTI-TARGET COOPERATIVE POWER ALLOCATION FOR JRC SYSTEM USING DEDICATED WAVEFORMS AND WORST-CASE CAPACITY OPTIMIZATION (34)

	Radar-only	Communication-only	Overall
Transmit powers (W)	$\mathbf{p}_{\rm tx}^{\rm rad} = \begin{bmatrix} 77.97 \\ 0 \\ 97.36 \\ 0 \\ 0 \end{bmatrix}$	$\mathbf{p}_{\rm tx}^{\rm com} = \begin{bmatrix} 0 \\ 40.7 \\ 1.45 \\ 41.63 \\ 40.86 \end{bmatrix}$	$\mathbf{p}_{\rm tx} = \begin{bmatrix} 77.97 \\ 40.70 \\ 98.81 \\ 41.63 \\ 40.86 \end{bmatrix}$
Total Power (W)	175.33	124.64	300
$\sqrt{\eta_{1,\rm achieve}}$ (m)	3.12	–	3.12
$\sqrt{\eta_{2,\rm achieve}}$ (m)	3.07	–	3.07
$\Re$ (bits/sec/Hz)	–	39.35	39.35

IX. CONCLUSION

In this paper, we discussed different power allocation schemes for distributed JRC MIMO systems that perform both radar and communication functions simultaneously. We exploited target localization error and Shannon capacity as the performance metrics for the evaluation of radar and communication performance, respectively. Then, we presented radar- and communication-centric resource allocation that serves as the baseline to evaluate the resource allocation for the cooperative JRC system. Two novel power allocation strategies for cooperative JRC systems were discussed. First, we presented the power allocation for the JRC systems that exploit shared waveforms for both radar and communication tasks. Next, we discussed the power allocation problem for the JRC systems that use a dedicated set of waveforms for radar and communication functions enabling the JRC system to change radar waveforms depending on the radar surveillance profile. Simulation results were presented to illustrate the superior performance of the proposed power allocation strategies.

REFERENCES

[1] H. Griffiths, S. Blunt, L. Cohen, and L. Savy, "Challenge problems in spectrum engineering and waveform diversity," in *Proc. IEEE Radar Conf.*, Ottawa, Canada, April–May 2013, pp. 1–5.

[2] C. Baylis, M. Fellows, L. Cohen, and R. J. Marks, "Solving the spectrum crisis: Intelligent, reconfigurable microwave transmitter amplifiers for cognitive radar," *IEEE Microw. Mag.*, vol. 15, no. 5, pp. 94–107, July-Aug. 2014.

[3] H. Griffiths, L. Cohen, S. Watts, E. Mokole, C. Baker, M. Wicks, and S. Blunt, "Radar spectrum engineering and management: Technical and regulatory issues," *Proc. IEEE*, vol. 103, no. 1, pp. 85–102, Jan. 2015.

[4] A. Ahmed, *Strategies for Radar-Communication Spectrum Sharing*, Ph.D. Dissertation, Temple Univ., PA, 2021.

[5] A. Ahmed, E. Aboutanios, and Y. D. Zhang, "Sensing-centric ISAC signal processing," in *Integrated Sensing and Communications*, F. Liu, C. Masouros, and Y. C. Eldar, Eds., chapter 7, pp. 179–209. Springer, 2023.

[6] E. Biglieri, *Principles of Cognitive Radio*, Cambridge University Press, 2012.

[7] C. Sturm, T. Zwick, and W. Wiesbeck, "An OFDM system concept for joint radar and communications operations," in *Proc. IEEE Veh. Technol. Conf.*, Barcelona, Spain, April 2009, pp. 1–5.

[8] D. W. Bliss, "Cooperative radar and communications signaling: The estimation and information theory odd couple," in *Proc. IEEE Radar Conf.*, Cincinnati, OH, May 2014, pp. 50–55.

[9] F. Paisana, N. Marchetti, and L. A. DaSilva, "Radar, TV and cellular bands: Which spectrum access techniques for which bands?," *Commun. Surveys & Tuts.*, vol. 16, no. 3, pp. 1193–1220, 2014.

[10] Z. Geng, H. Deng, and B. Himed, "Adaptive radar beamforming for interference mitigation in radar-wireless spectrum sharing," *IEEE Signal Process. Lett.*, vol. 22, no. 4, pp. 484–488, April 2015.

[11] K.-W. Huang, M. Bica, U. Mitra, and V. Koivunen, "Radar waveform design in spectrum sharing environment: Coexistence and cognition," in *Proc. IEEE Radar Conf.*, Johannesburg, South Africa, May 2015, pp. 1698–1703.

[12] S. D. Blunt, M. R. Cook, and J. Stiles, "Embedding information into radar emissions via waveform implementation," in

Proc. Int. Waveform Diversity and Design Conf., Niagara Falls, Canada, Aug. 2010, pp. 195–199.

[13] J. Euziere, R. Guinvarc'h, M. Lesturgie, B. Uguen, and R. Gillard, "Dual function radar communication time-modulated array," in *Proc. Int. Radar Conf.*, Cincinnati, OH, Oct. 2014, pp. 1–4.

[14] A. Hassanien, M. G. Amin, Y. D. Zhang, and F. Ahmad, "Dual-function radar-communications: Information embedding using sidelobe control and waveform diversity," *IEEE Trans. Signal Process.*, vol. 64, no. 8, pp. 2168–2181, April 2016.

[15] A. Hassanien, M. G. Amin, Y. D. Zhang, and F. Ahmad, "Signaling strategies for dual-function radar communications: An overview," *IEEE Aerosp. Electron. Syst. Mag.*, vol. 31, no. 10, pp. 36–45, Oct. 2016.

[16] A. Ahmed, Y. D. Zhang, and B. Himed, "Multi-user dual-function radar-communications exploiting sidelobe control and waveform diversity," in *Proc. IEEE Radar Conf.*, Oklahoma City, OK, April 2018, pp. 698–702.

[17] A. Ahmed, Y. D. Zhang, and Y. Gu, "Dual-function radar-communications using QAM-based sidelobe modulation," *Digital Signal Process.*, vol. 82, pp. 166–174, Nov. 2018.

[18] A. Ahmed, Y. Gu, D. Silage, and Y. D. Zhang, "Power-efficient multi-user dual-function radar-communications," in *Proc. IEEE Int. Workshop on Signal Process. Advances in Wireless Commun.*, Kalamata, Greece, June 2018.

[19] J. Qian, Z. Liu, K. Wang, N. Fu, and J. Wang, "Transmission design for radar and communication spectrum sharing enhancement," *IEEE Trans. Veh. Technol.*, vol. 72, no. 2, pp. 2723–2727, Feb. 2023.

[20] Bin Liao, Xue Xiong, and Zhi Quan, "Robust beamforming design for dual-function radar-communication system," *IEEE Trans. Veh. Technol.*, vol. 72, no. 6, pp. 7508–7516, Jan. 2023.

[21] L. Lin, H. Zheng, C. Zhou, S. He, and Z. Shi, "Nonorthogonal waveform assisted DOA estimation for joint MIMO sensing and communication," *EURASIP J. Adv. Signal Process.*, vol. 2023, no. 1, pp. 1–19, Feb. 2023.

[22] Z. Xu and A. Petropulu, "A bandwidth efficient dual-function radar communication system based on a MIMO radar using OFDM waveforms," *IEEE Trans. Signal Process.*, vol. 71, pp. 401–416, 2023.

[23] L. Lin, H. Zheng, C. Zhou, and Z. Shi, "Channel covariance matrix construction for DOA estimation with limited communication symbols," in *Proc. IEEE Radar Conf.*, San Antonio, TX, May 2023, pp. 1–5.

[24] A. Ahmed, Y. D. Zhang, A. Hassanien, and B. Himed, "OFDM-based joint radar-communication system: Optimal sub-carrier allocation and power distribution by exploiting mutual information," in *Proc. Asilomar Conf. Signals, Syst., and Comput.*, Pacific Grove, CA, Nov. 2019, pp. 559–563.

[25] M. Bică and V. Koivunen, "Multicarrier radar-communications waveform design for RF convergence and coexistence," in *Proc. IEEE Intl. Conf. Acoustics, Speech, Signal Process.*, Brighton, UK, May 2019, pp. 7780–7784.

[26] F. Wang, H. Li, and M. A. Govoni, "Power allocation and co-design of multicarrier communication and radar systems for spectral coexistence," *IEEE Trans. Signal Process.*, vol. 67, no. 14, pp. 3818–3831, July 2019.

[27] A. Ahmed, Y. D. Zhang, and A. Hassanien, "Joint radar-communications exploiting optimized OFDM waveforms," *Remote Sensing*, vol. 13, no. 21, Oct. 2021.

[28] B. Hong, W-Q. Wang, and C-C. Liu, "Interference utilization for spectrum sharing radar-communication systems," *IEEE Trans. Veh. Technol.*, vol. 70, no. 8, pp. 8304–8308, June 2021.

[29] A. Ahmed, Y. D. Zhang, and B. Himed, "Distributed dual-function radar-communication MIMO system with optimized resource allocation," in *Proc. IEEE Radar Conf.*, Boston, MA, April 2019, pp. 1–5.

[30] A. Ahmed, Y. D. Zhang, and B. Himed, "System and method for distributed dual-function radar-communication," U.S. Patent 11598841B1, March 7, 2023.

[31] C. Shi, Y. Wang, F. Wang, S. Salous, and J. Zhou, "Power resource allocation scheme for distributed MIMO dual-function radar-communication system based on low probability of intercept," *Digital Signal Process.*, vol. 106, no. 102850, pp. 1–12, Nov. 2020.

[32] B. Shang, V. Marojevic, Y. Yi, A. Abdalla, and L. Liu, "Spectrum sharing for UAV communications: Spatial spectrum sensing and open issues," *IEEE Veh. Technol. Mag.*, vol. 15, no. 2, pp. 104–112, June 2020.

[33] A. Ahmed, S. Zhang, and Y. D. Zhang, "Antenna selection strategy for transmit beamforming-based joint radar-communication system," *Digital Signal Process.*, vol. 105, pp. 102768, Oct. 2020.

[34] A. Ahmed, S. Zhang, and Y. D. Zhang, "Optimized sensor selection for joint radar-communication systems," in *Proc. IEEE Intl. Conf. Acoustics, Speech, Signal Process.*, Barcelona, Spain, May 2020, pp. 4682–4686.

[35] L. Wu, K. V. Mishra, M. R. B. Shankar, and B. Ottersten, "Heterogeneously-distributed joint radar communications: Bayesian resource allocation," in *Proc. IEEE Int. Workshop Signal Process. Adv. Wireless Commun. (SPAWC)*, Lucca, Italy, Sept. 2021, pp. 506–510.

[36] A. M. Haimovich, R. S. Blum, and L. J. Cimini, "MIMO radar with widely separated antennas," *IEEE Signal Process. Mag.*, vol. 25, no. 1, pp. 116–129, Dec. 2008.

[37] H. Godrich, A. M. Haimovich, and R. S. Blum, "Target localization accuracy gain in MIMO radar-based systems," *IEEE Trans. Inf. Theory*, vol. 56, no. 6, pp. 2783–2803, June 2010.

[38] H. Godrich, A. P. Petropulu, and H. V. Poor, "Power allocation strategies for target localization in distributed multiple-radar architectures," *IEEE Trans. Signal Process.*, vol. 59, no. 7, pp. 3226–3240, July 2011.

[39] M. Skolnik, *Introduction to Radar Systems,* 3rd Ed., McGraw-Hill, 2001.

[40] B. Friedlander, "Waveform design for MIMO radars," *IEEE Trans. Aerosp. Electron. Syst.*, vol. 43, no. 3, pp. 1227–1238, July 2007.

[41] H. He, P. Stoica, and J. Li, "Designing unimodular sequence sets with good correlations–Including an application to MIMO radar," *IEEE Trans. Signal Process.*, vol. 57, no. 11, pp. 4391–4405, Nov. 2009.

[42] Y. Wang, W. Li, Q. Sun, and G. Huang, "Robust joint design of transmit waveform and receive filter for MIMO radar space-time adaptive processing with signal-dependent interferences," *IET Radar Sonar Navig.*, vol. 11, no. 8, pp. 1321–1332, June 2017.

[43] B. Ristic, S. Arulampalam, and N. Gordon, *Beyond the Kalman Filter: Particle Filters for Tracking Applications*, Artech House, 2003.

[44] F. Sohrabi, Z. Chen, and W. Yu, "Deep active learning approach to adaptive beamforming for mmWave initial alignment," *IEEE J. Sel. Areas Commun.*, vol. 39, no. 8, pp. 2347–2360, Aug. 2021.

[45] J. Walrand and P. Varaiya, "Wireless networks," in *High-Performance Communication Networks, 2nd Ed.*, J. Walrand and P. Varaiya, Eds., pp. 305–361. Morgan Kaufmann, 2000.

[46] J. Li and P. Stoica, *MIMO Radar Signal Processing*, Wiley-IEEE Press, 2008.

[47] T. M. Cover and J. A. Thomas, *Elements of Information Theory*, Wiley-Interscience, 2006.

[48] G. D. Forney and G. Ungerboeck, "Modulation and coding for linear Gaussian channels," *IEEE Trans. Inf. Theory*, vol. 44, no. 6, pp. 2384–2415, Oct. 1998.

[49] M. Grant and S. Boyd, "CVX: MATLAB software for disciplined convex programming, version 2.1," http://cvxr.com/cvx, March 2014.

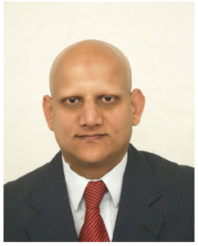

Ammar Ahmed (Member, IEEE) received Ph.D. degree from Temple University, Philadelphia, USA, in 2021.

Dr. Ahmed is currently a Radar Signal Processing Engineer at Aptiv, Agoura Hills, CA, USA. His research interests are in signal processing, data analysis, optimization, and radar systems. He served as a Program Co-Chair for the 2021 IEEE Signal Processing in Medicine and Biology Symposium and a General Co-Chair for the 2022 IEEE Signal Processing in Medicine and Biology Symposium. He is serving as a General Co-Chair for the 2023 IEEE Signal Processing in Medicine and Biology Symposium.

Yimin D. Zhang (Fellow, IEEE) received the Ph.D. degree from the University of Tsukuba, Tsukuba, Japan, in 1988.

He is currently an Associate Professor with the Department of Electrical and Computer Engineering, Temple University, Philadelphia, PA, USA. His research interests include array signal processing, compressive sensing, machine learning, information theory, convex optimization, and time-frequency analysis with applications to radar, wireless communications, and satellite navigation.

Dr. Zhang is a Senior Area Editor for *IEEE Transactions on Signal Processing* and an Associate Editor for *Signal Processing*. He was an Associate Editor for *IEEE Transactions on Signal Processing*, *IEEE Transactions on Aerospace and Electronic Systems*, *IEEE Signal Processing Letters*, and *Journal of the Franklin Institute*. He was a Technical Co-Chair of the 2018 IEEE Sensor Array and Multichannel Signal Processing Workshop. He was the recipient of the 2016 IET Radar, Sonar & Navigation Premium Award, the 2017 IEEE Aerospace and Electronic Systems Society Harry Rowe Mimno Award, the 2019 IET Communications Premium Award, and the 2021 EURASIP Best Paper Award for Signal Processing. He coauthored two papers that respectively received the 2018 and 2021 IEEE Signal Processing Society Young Author Best Paper Awards. Dr. Zhang is a 2024 IEEE Signal Processing Society Distinguished Lecturer. He is a Fellow of SPIE.